Journal of Renewable Materials

Tech Science Press

DOI: 10.32604/jrm.2022.022192

ARTICLE

Analysis of the Relationship between Mechanical Properties and Pore Structure of MSW Incineration Bottom Ash Fine Aggregate Concrete after Freeze-Thaw Cycles Based on the Gray Theory

Peng Zhang[1], Dongsheng Shi[1,*], Ping Han[1,2] and Wenchao Jiang[1,3]

[1]School of Civil Engineering, Inner Mongolia University of Technology, Hohhot, 010000, China

[2]Xingtai Construction Group Co., Ltd., Hohhot, 010000, China

[3]Inner Mongolia Electric Power (Group) Company Limited Mengdian Project Construction and Management Branch, Hohhot, 010000, China

[*]Corresponding Author: Dongsheng Shi. Email: shids@imut.edu.cn

Received: 25 February 2022 Accepted: 04 May 2022

ABSTRACT

The destruction of concrete building materials in severely cold regions of the north is more severely affected by freeze-thaw cycles, and the relationship between the mechanical properties and pore structure of concrete with fine aggregate from municipal solid waste (MSW) incineration bottom ash after freeze-thaw cycles is analyzed under the degree of freeze-thaw hazard variation. In this paper, the gray correlation method is used to calculate the correlation between the relative dynamic elastic modulus, compressive strength, and microscopic porosity parameters to speculate on the most important factors affecting their changes. The GM (1,1) model was established based on the compressive strength of the waste incineration ash aggregate concrete, the relative error between the simulated and actual values in the model was less than 5%, and the accuracy of the model was level 1, indicating that the GM (1,1) model can well reflect the change in the compressive strength of the MSW incineration bottom ash aggregate concrete during freeze-thaw cycles. Using the gray correlation method, the correlation between the relative dynamic elastic modulus, compressive strength, air content, specific surface area, pore spacing coefficient, and pore average chord length was calculated, and the pore spacing coefficient and pore average chord length were determined to be highly correlated with each other. This determination can help analyze and infer the deterioration mechanism of concrete subject to freeze-thaw cycles. These results can provide a theoretical basis for guiding the engineering practice of concrete with fine aggregates of household bottom ash in the northern cold region.

KEYWORDS

Municipal solid waste incineration bottom ash; concrete; gray system theory; mechanical properties; pore structure

1 Introduction

With the widespread adoption of municipal waste incineration, the amount of bottom ash generated by incineration is also increasing [1–3]. The common methods implemented for MSW management are landfilling, composting, and incineration [4]. Use of municipal solid waste inert as a powerful replacement of fine aggregate in mortar cube [5]. Mortar made from concrete slurry waste (CSW) and municipal solid waste incineration bottom ash (MSWIBA) could be recycled into cold bonded lightweight aggregates (CBLA) [6]. The amount of domestic waste removed in 2020 was 235 million tons [7], the amount of MSW incinerated harmlessly in 2020 was approximately 146 million tons [8], and the percentage of MSW treated by incineration was approximately 62.1%. At present, the resource utilization of MSW incineration bottom ash in the field of construction engineering mainly includes the following aspects: replacing pavement base material [9]; foam glass with good performance was prepared by using MSW incineration bottom ash as the main raw material [10], etc. Currently, our team has studied the carbonation and resistance to chloride-ion penetration of fine aggregate concrete from MSW incineration and has tested the mechanical properties simulated by engineering members made from MSW incineration ash concrete under simulated construction conditions [11,12]. The test results have shown that the radioactivity of the test ash is within the safe range and can be used for the preparation of construction materials without any restriction and without any impact on environmental safety [13]. The results of the solid toxic substances leaching tests from MSW incineration bottom ash meet the relevant regulations and can be used as concrete aggregates [14]. To study the relationship between the mechanical properties and porosity characteristics of the material and to reasonably match the distribution of the solid phase and porosity, it is urgent to prepare porous materials with high porosity and high strength [15].

In 1982, Chinese scholar Professor Deng Julong developed gray systems theory, which is a new approach to studying uncertainty in systems with little data and poor information [16,17]. Information incompleteness, as the main feature of an uncertain system, has the following characteristics. a) Incomplete element information, b) incomplete structural information, c) incomplete boundary information, and d) incomplete operational behavior information [18]. Gray system theory uses the gray system method and modeling technology, through the analysis of a small amount of “known information”, to identify the key information and relationships in the system and to predict the future development trend of the system [19,20]. GM has differences and compatibility, GM structure has elasticity and diversity, GM is a constant coefficient in nature, and its parameter distribution is gray [21]. As a very active branch of gray system theory, gray correlation analysis is mainly based on the similarity of the series curve geometry to determine whether the connection between different series is strong or not, and the closer the geometry is, the greater the correlation.

As one of the three major factors of concrete damage, freeze-thaw action plays an important role in the research field of concrete durability [22]. In Northern China, the freeze-thaw cycle is the main factor for the decline in structural durability [23]. In the United States, freeze-thaw has become the cause of reinforced concrete structures in cold regions such as North Dakota main factor of deterioration of mechanical properties [24].

This paper focuses on the prediction of the compressive strength of household waste incineration ash aggregate concrete and normal concrete (control group) using the mean GM (1,1) model with the gray theory system and the decay of the compressive strength with an increase in the number of freeze-thaw cycles to predict the compressive strength values in the future. From the microscopic point of view, the pore parameters, such as air content, specific surface area, pore spacing coefficient, and average pores chord length, were analyzed by the gray correlation method to determine the correlation and influence on the compressive strength and relative dynamic elastic modulus of concrete after freeze-thaw cycles to determine the most influential factors on the freezing performance of concrete and to guide engineering practice.

2 Experimental Overview and Results

2.1 Test Material and Concrete Mix Ratio

The proportions used in this test were designed by the volumetric method, and the composition of the concrete is outlined below. The MSW incineration bottom ash was from a waste treatment plant in Hohhot, Inner Mongolia, and had a chemical composition similar to that of natural sand, consisting of some oxides. The main chemical composition of the ash from MSW is listed in Table 1. The sand was natural washed sand from the Dahei River in Hohhot, Inner Mongolia. The gravel was first grade crushed granite from Daqing Mountain, Hohhot, Inner Mongolia, with a particle size of 5~20 mm. The basic performance indicators of aggregates are listed in Table 2. The cement was P·O 42.5 grade ordinary silicate cement produced by Jidong Cement Plant in Hohhot. The silica fume was from Lingshou County, Shijiazhuang. The water-reducing agent was polycarboxylic acid high-efficiency water reducing agent, which has the characteristics of low admixture and a high water reducing rate, and the water reducing rate was more than 35% when the admixture was approximately 1%. The tested compounds are listed in Table 3. Three water-cement ratios of 0.2, 0.4, and 0.6 were selected to cover high strength, medium strength, and ordinary strength concrete, and three sand replacement rates (Srr) of 0%, 25%, and 50% were set under each water-cement ratio.

Table 1: Chemical composition content

Material	Chemical composition content (%)				
	SiO_2	CaO	Fe_2O_3	MnO	Al_2O_3
MSW	48.26	16.49	4.60	0.09	8.89

Table 2: Aggregate basic performance indicators

Indicators	MSW	Natural sand	Gravel
Crushing index value/%	69.0	21.0	9.9
Void ratio/%	22.0	9.8	—
Water content/%	11.0	2.0	0.3
Water absorption rate/%	10.4	1.5	0.6
Apparent density/(kg/m^3)	2450	2660	2760
Packing density/(kg/m^3)	1020	1460	1310
Fineness modulus	2.4	2.6	—

Table 3: Mix ratio of fine aggregate concrete with MSW incineration ash

m_w/m_b	Sand replacement rate (%)	Concrete mix ratio (kg/m^3)					
		Aggregate	Sand rate	Cementitious material	Water	Ash	Water reducing agent
0.2	0	1425.8	49.1%	825.0	154.1	0	10.89
	25	1250.9	42.0%	825.0	153.0	161.1	11.97
	50	1075.9	32.5%	825.0	152.0	322.3	13.04
0.4	0	1762.7	44.1%	425.0	167.5	0	2.55
	25	1568.0	37.1%	425.0	167.2	179.0	2.76
	50	1373.9	28.3%	425.0	167.0	357.9	2.98
0.6	0	1806.8	41.1%	300.0	178.8	0	1.20
	25	1621.2	34.4%	300.0	178.2	171.0	1.80
	50	1435.5	25.9%	300.0	177.6	342.0	2.40

2.2 Test Method

(1) Freeze-thaw test method

The test was by the "Standard for long-term performance and durability of ordinary concrete test methods" (GB/T 50082-2009) using a rapid freeze-thaw method. Specifically, the cube specimen of $100 \times 100 \times 100\ mm^3$ was used to measure the freezing and thawing times that the concrete can withstand. The relative dynamic modulus of elasticity of MSW incineration bottom ash fine aggregate concrete was measured after every 25 freeze-thaw cycles and the compressive strength of the specimens was measured after 0, 25, 50, 75, 100, 200, and 300 freeze-thaw cycles to analyze and evaluate the freezing resistance of the concrete with ash from MSW incineration. The relative dynamic modulus of elasticity and the mass loss rate is nondestructive methods, so the damage to the concrete specimens can be observed and evaluated in overall freeze-thaw cycles.

(2) Mechanical properties test method

The test was carried out according to the requirements of the "Standard for Mechanical Properties of General Concrete" (GB/T 50081-2002). The cube specimen with the size of $100 \times 100 \times 100\ mm^3$ is made to test the compressive strength of concrete. The final cube compressive strength of the test is the average value of the pressure measured by the three specimens, and the test data is accurate to 0.1 Mpa. Since the specimen used in the test is a non-standard cube specimen, the cube compressive strength value obtained according to the standard requirement needs to be multiplied by a size conversion coefficient of 0.95.

(3) Optical method of measuring the pore structure

This test uses the optical method to measure the pore structure of the concrete with fine aggregate from MSW incineration. The test instrument was Rapid Air 457. The Rapid Air 457 concrete pore structure analyzer is manufactured by Concrete Experts International in Denmark. The Rapid Air 457 includes an automated analysis system, a computer control unit (PC) and a color monitor, a camera lens and a microscope objective mounted on a mobile bench, a user-friendly analysis software running under Microsoft Windows. a pore structure analyzer for hardened concrete, which can quickly analyze the pore surface area, air content, bubble spacing coefficient, bubble average chord length, and other parameters and can be used to evaluate the frost resistance of concrete from the side by the bubbles and pores [25]. After the number of freeze-thaw cycles of MSW incineration ash fine aggregate concrete is reached, the cube test block of $100 \times 100 \times 100\ mm^3$ is cut by a cutting machine, and the test block is cut into $100 \times 100 \times 10\ mm^3$ thin slices. In the grinding process, 320 mesh, 600 mesh, 800 mesh, 1200 mesh silicon carbide, and water 1:1 were used to prepare the solution. The solution was poured into the disc regularly according to the amount of mesh from low to high, and the time interval was about 10 min until the surface of the specimen was smooth and smooth. After grinding, clean and mark the specimen. Melt Vaseline into liquid and white zinc oxide powder according to the proportion of 1:1 to the viscous solution, use knife evenly spread on the surface of the test piece (black side of the surface). Then a knife is used to gently scrape the mixed solution on the surface of the test piece, and a layer of mineral oil is smeared on the surface of the test piece. Finally, the mineral oil is wiped clean and the preparation of the test piece is completed. Subsequently, the micro-pore structure was tested.

2.3 Experimental Results

The compressive strength values of the concrete with fine aggregates from MSW incineration bottom ash for different numbers of freeze-thaw cycles are listed in Table 4. The values of the relative dynamic elastic modulus of concrete with fine aggregates from MSW incineration are listed in Table 5. The microscopic pore structure characteristic parameters of concrete with fine aggregates from MSW incineration are listed in Table 6.

Table 4: Cube compressive strength of fine aggregate concrete from MSW incineration ash under different freeze-thaw cycles/MPa

m_w/m_b	Sand replacement rate (%)	Number of freeze-thaw cycles (cycles)					
		0	25	50	100	200	300
0.2	0	83.78	73.29	62.47	59.50	59.25	56.03
	25	64.63	64.43	56.07	55.12	52.41	49.92
	50	54.75	51.23	50.96	46.01	45.85	45.74
0.4	0	51.76	43.78	35.84	31.36	—	—
	25	44.76	37.36	33.66	27.92	—	—
	50	43.33	38.51	35.52	33.70	29.22	26.43
0.6	0	36.10	28.24	22.32	—	—	—
	25	28.35	21.96	21.28	—	—	—
	50	29.70	27.72	24.99	20.24	—	—

Note: Unfilled data in the table indicate that the test specimen reached the freeze-thaw test stopping conditions and the test was stopped.

Table 5: Variation of relative dynamic elastic modulus of fine aggregate concrete with MSW incineration ash

m_w/m_b	Sand replacement rate (%)	Number of freeze-thaw cycles (cycles)				
		0	50	100	200	300
0.2	0	100	99.1	98.3	98.2	97.2
	25	100	99.6	99.2	97.0	95.2
	50	100	98.7	98.2	98.0	96.2
0.4	0	100	86.1	67.6	—	—
	25	100	89.3	66.8	—	—
	50	100	97.7	94.3	92.3	88.6
0.6	0	100	80.0	10.0	—	—
	25	100	67.1	—	—	—
	50	100	91.2	87.4	—	—

Note: Unfilled data in the table indicate that the test specimen reached the freeze-thaw test stopping conditions and the test was stopped.

3 Gray Theory of Strength under Freeze-Thaw Cycles

Many prediction models are using gray system theory, and since the GM (1, N) model considers many factors, there is also a correlation between each factor. Therefore, it is difficult for the analyst to strip out the most direct factors affecting the test from the model. After many studies, a better effect was found using the single-factor model GM (1,1), meaning a first-order, one-variable gray model, and this model is a basic and comprehensive prediction model [26]. According to the compressive strength values of concrete with fine aggregates from MSW incineration bottom ash, the GM (1,1) model was established to predict the change in the compressive strength with the increase in the number of freeze-thaw cycles and to analyze and evaluate the frost resistance of concrete.

Table 6: Characteristic parameters of the micropore structure of fine aggregate concrete with MSW incineration ash

m_w/m_b	Sand replacement rate (%)	Freeze-thaw cycles (cycles)	Air content (%)	Specific surface area (mm^{-1})	Pore spacing coefficient (mm)	Average pore chord length (mm)
0.2	0	0	1.04	25.78	0.384	0.125
		50	1.64	42.83	0.358	0.097
		100	1.77	40.38	0.273	0.093
		200	2.15	37.11	0.121	0.077
		300	2.26	30.19	0.218	0.061
	25	0	1.24	42.39	0.254	0.114
		50	1.30	68.13	0.162	0.074
		100	1.53	59.68	0.171	0.083
		200	2.32	56.97	0.105	0.072
		300	2.53	44.61	0.231	0.122
	50	0	1.63	49.56	0.165	0.101
		50	1.70	86.18	0.093	0.046
		100	1.68	79.31	0.090	0.053
		200	3.00	65.66	0.102	0.064
		300	3.25	56.86	0.244	0.093
0.4	0	0	1.14	49.56	0.384	0.122
		25	1.82	86.18	0.072	0.041
		50	1.90	79.31	0.212	0.051
		75	2.01	65.66	0.263	0.029
		100	2.17	56.86	0.348	0.103
	25	0	1.25	31.49	0.352	0.153
		25	1.36	67.93	0.132	0.059
		50	1.99	57.22	0.144	0.068
		75	2.46	47.46	0.169	0.086
		100	2.71	32.87	0.256	0.122
	50	0	1.52	28.00	0.312	0.112
		50	1.49	72.05	0.282	0.058
		100	1.81	62.36	0.252	0.058
		200	1.93	46.17	0.081	0.083
		300	2.29	52.84	0.301	0.130

(Continued)

Table 6 (continued)

m_w/m_b	Sand replacement rate (%)	Freeze-thaw cycles (cycles)	Air content (%)	Specific surface area (mm^{-1})	Pore spacing coefficient (mm)	Average pore chord length (mm)
0.6	0	0	1.34	63.46	0.214	0.092
		25	1.46	82.40	0.114	0.049
		50	1.66	47.50	0.087	0.042
	25	0	1.55	31.33	0.321	0.121
		25	1.63	49.42	0.160	0.071
		50	1.99	40.81	0.058	0.042
	50	0	1.73	47.42	0.382	0.114
		25	1.85	55.86	0.100	0.066
		50	1.70	57.83	0.144	0.072
		75	1.95	47.05	0.163	0.093
		100	2.60	38.71	0.200	0.124
		125	2.87	34.13	0.212	0.152

3.1 Establishing the GM (1,1) Model

Set sequence

$$X^{(0)} = (x^{(0)}(1),\ x^{(0)}(2),\ \cdots,\ x^{(0)}(n)) \tag{1}$$

where $x^{(0)}(k) \geq 0$, k = 1,2,…,n. X(1) is the 1-AGO sequence of X(0), i.e., the accumulation of (1) yields the generating series.

$$X^{(1)} = (x^{(1)}(1),\ x_k^{(1)}(2),\ \cdots,\ x^{(1)}(n)) \tag{2}$$

where, $x^{(1)}(k) = \sum_{i=1} x^{(0)}(i)$, k = 1,2,…,n

$$Z^{(1)} = (z^{(1)}(2),\ z^{(1)}(3),\ \cdots,\ z^{(1)}(n)) \tag{3}$$

where, $z^{(1)}(k) = \frac{1}{2}(x^{(1)}(k) + x^{(1)}(k-1))$, k = 2,3,…,n,

The mean value form of the GM (1,1) model is obtained:

$$x^{(0)}(k) + az^{(1)}(k) = b \tag{4}$$

Derivation of Eq. (4) with respect to time t yields the whitening equation for the GM (1,1) model:

$$\frac{dx^{(1)}}{dt} + ax^{(1)} = b \tag{5}$$

The parameter vector $\hat{a} = [a,\ b]^T$ in Eq. (5) is estimated by least squares using Eq. (6):

$$\hat{a} = (B^T B)^{-1} B^T Y \tag{6}$$

where $Y = \begin{bmatrix} x^{(0)}(2) \\ x^{(0)}(3) \\ \vdots \\ x^{(0)}(n) \end{bmatrix}, B = \begin{bmatrix} -z^{(1)}(2) & 1 \\ -z^{(1)}(3) & 1 \\ \vdots & 1 \\ -z^{(1)}(n) & 1 \end{bmatrix}$

The solution of the whitening equation of the GM (1,1) model, i.e., the time response equation, is obtained as

$$\hat{x}^{(1)}(k) = \left(x^{(0)}(1) - \frac{b}{a}\right)e^{-a(k-1)} + \frac{b}{a} \quad k = 1, 2, \ldots, n \tag{7}$$

Then, the simulated values of the original data are

$$\hat{x}^{(0)}(k) = (1 - e^{a})\left(x^{(0)}(1) - \frac{b}{a}\right)e^{-a(k-1)} \quad k = 1, 2, \ldots, n \tag{8}$$

where a and b are unknown parameters, –a is the development coefficient, which reflects the development trend of $\hat{x}^{(1)}$ and $\hat{x}^{(0)}$ and b is the gray effect quantity, which is used to reflect the change relationship of the data.

3.2 Model Accuracy Test

Model residuals

$$\varepsilon^{(0)}(k) = x^{(0)}(k) - \hat{x}^{(0)}(k) \quad k = 1, 2, \ldots, n \tag{9}$$

Means and variances of the original series

$$\bar{x} = \frac{1}{n}\sum_{k=1}^{n} x^{(0)}(k) \tag{10}$$

$$S_1^2 = \frac{1}{n}\sum_{k=1}^{n}\left(x^{(0)}(k) - \bar{x}\right)^2 \tag{11}$$

Means and variances of the residual series

$$\bar{\varepsilon} = \frac{1}{n}\sum_{k=1}^{n} \varepsilon(k) \tag{12}$$

$$S_2^2 = \frac{1}{n}\sum_{k=1}^{n}\left(\varepsilon(k) - \bar{\varepsilon}\right)^2 \tag{13}$$

Mean-variance ratio

$$C = \frac{s_2}{s_1} \tag{14}$$

The small error probability p

$$p = P(|\varepsilon(k) - \bar{\varepsilon}| \prec 0.6745 S_1) \tag{15}$$

The smaller the C-value is, the better the model; in general, the C-value should be less than 0.35, and the maximum should not exceed 0.65. Another index is needed to evaluate the accuracy of the model: the larger the small error probability p value is, the higher the accuracy of the model; in general, the p value should be greater than 0.95, and the minimum should not be less than 0.70. According to the above conditions, the model prediction accuracy is divided into four levels, as see Table 7.

Table 7: Accuracy grade of the gray theory model

Accuracy class	Mean square error ratio C	Probability of small error p
Level 1 (good)	$C \leqq 0.35$	$p \geqq 0.95$
Level 2 (qualified)	$0.35 < C \leqq 0.50$	$0.80 \leqq p < 0.95$
Level 3 (barely)	$0.50 < C \leqq 0.65$	$0.70 \leqq p < 0.80$
Level 4 (unqualified)	$0.65 < C$	$p < 0.70$

3.3 Compressive Strength Prediction and Analysis

In this prediction, the compressive strength of MSW incineration bottom ash fine aggregate concrete and ordinary concrete at 0, 25, 50, 100, 200, and 300 freeze-thaw cycles are the original series X(0), and the GM (1,1) prediction model is established according to the method described in 3.1, and the calculation steps are as follows:

(1) The measured compressive strength values of each group of specimens after freeze-thaw cycles were accumulated and processed to obtain the 1-AGO series, as listed in Table 8.

Table 8: Sequence 1-AGO

m_w/m_b	Sand replacement rate (%)	Cumulative sequence	Compressive strength under different freeze-thaw cycles (MPa)					
			0 cycles	25 cycles	50 cycles	100 cycles	200 cycles	300 cycles
0.2	0	$X_1^{(1)}$	83.8	157.1	219.5	279.0	338.3	394.3
	25	$X_2^{(1)}$	64.6	129.1	185.1	240.3	292.7	342.6
	50	$X_3^{(1)}$	54.8	106.0	156.9	203.0	248.8	294.5
0.4	0	$X_5^{(1)}$	51.8	95.5	131.4	162.7	—	—
	25	$X_6^{(1)}$	44.8	82.1	115.8	143.7	—	—
	50	$X_4^{(1)}$	43.3	81.8	117.4	151.1	180.3	206.7
0.6	0	$X_7^{(1)}$	36.1	64.3	86.7	—	—	—
	25	$X_8^{(1)}$	28.4	50.3	71.6	—	—	—
	50	$X_9^{(1)}$	29.7	57.4	82.4	102.7	—	—

Note: Unfilled data in the table indicate that the test specimen reached the freeze-thaw test stopping conditions and the test was stopped.

(2) Using Eqs. (4) and (6), based on the principle of least squares, the development coefficient a and the gray effect b were calculated to obtain the solution (time response series) of the whitening equation given by Eqs. (2)–(5), i.e., the gray prediction model, as listed in Table 9.

(3) Using the gray prediction model for forecasting, the obtained results are listed in Fig. 1.

After obtaining the prediction results of the GM (1,1) model, the accuracy of the model was tested according to the method described in Section 2.2, and the results obtained are listed in Table 10.

Table 9: Gray prediction model

m_w/m_b	Sand replacement rate (%)	Development coefficient a	Gray effect b	Average simulation relative error
	0	0.062494	77.518842	3.65%
0.2	25	0.059800	68.156400	2.10%
	50	0.033891	53.985974	2.01%
	0	0.170110	55.941889	1.55%
0.4	25	0.141414	46.750427	1.81%
	50	0.092291	44.776500	1.60%
	0	0.234177	40.000380	0.35%
0.6	25	0.031452	23.197021	0.01%
	50	0.151402	34.713195	2.35%

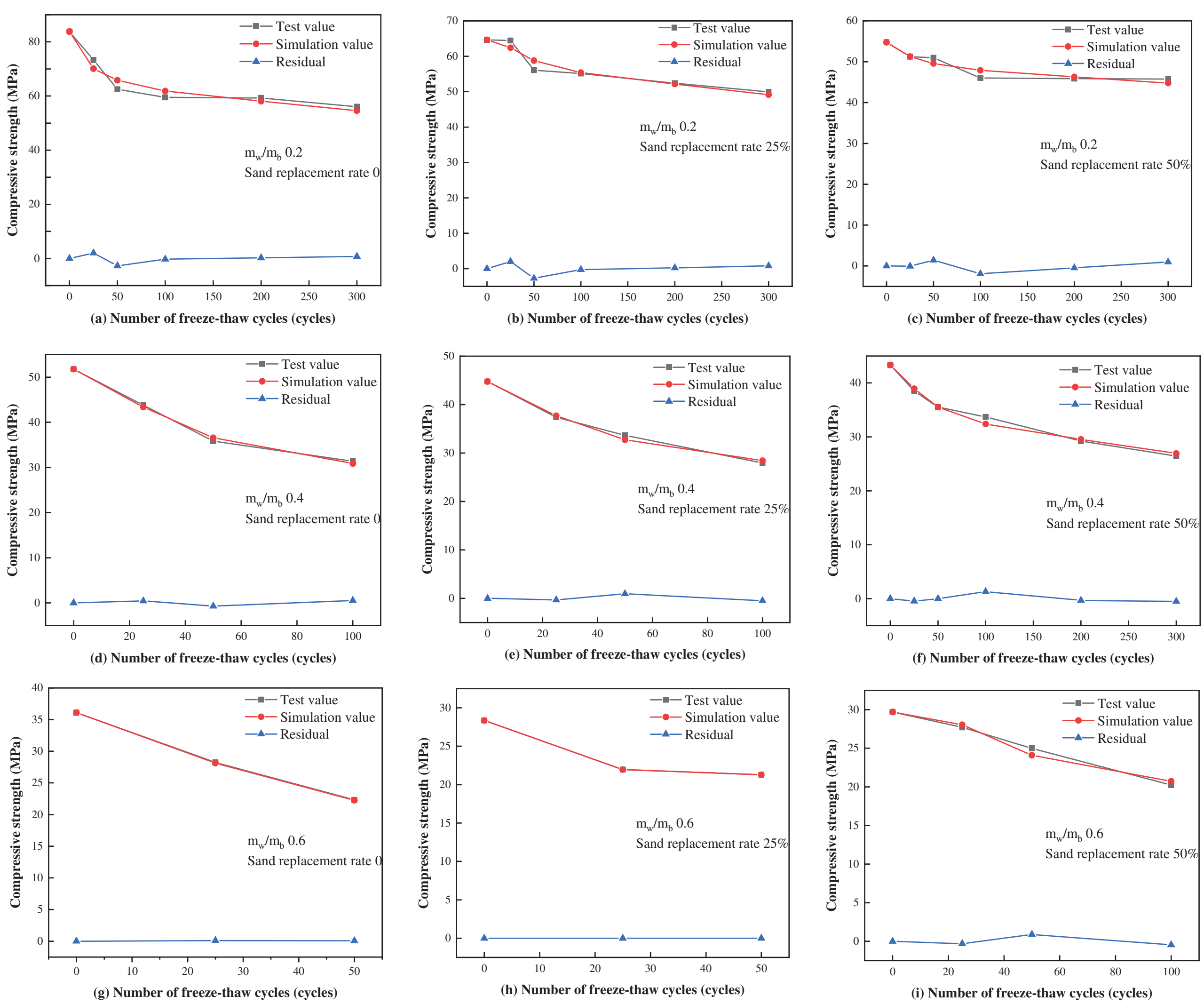

Figure 1: Calculation results of the GM (1,1) model

Table 10: Model precision

m_w/m_b	Sand replacement rate (%)	Mean square error ratio C	Small probability error p	Accuracy class
0.2	0	0.05745	1	Level 1
	25	0.08645	1	Level 1
	50	0.31944	1	Level 1
0.4	0	0.06312	1	Level 1
	25	0.09072	1	Level 1
	50	0.09715	1	Level 1
0.6	0	0.00805	1	Level 1
	25	0.00148	1	Level 1
	50	0.14861	1	Level 1

Fig. 1 shows that the model predicts the compressive strength of concrete with fine aggregate from MSW incineration after freeze-thaw cycles using the GM (1,1) model, regardless of whether it is mixed with MSW incineration bottom ash. The model predictions are better, and the relative errors are less than 5% when comparing the test values with the simulated values, which means that the model can predict the compressive strength values of concrete after freeze-thaw cycles well. As seen in Table 13, the mean squared error ratio C obtained from the actual and predicted values of each group of tests is less than 0.35, the small probability error is 1, which is greater than 0.95, and the prediction accuracy of each group of models is first class, which indicates that the compressive strength of concrete with fine aggregate from MSW incineration bottom ash in freeze-thaw cycles can be effectively predicted using the mean GM (1,1) model, which can accurately reflect the frost resistance of concrete in freeze-thaw cycles.

4 Analysis of the Relationship between Pore Structure and Macroscopic Performance Based on Gray Correlation

The test results show that with the increasing number of freeze-thaw cycles, the relative dynamic modulus of elasticity of concrete with fine aggregate from MSW incineration gradually decreases, and the compressive strength also gradually decreases with the increasing number of freeze-thaw cycles; through the determination of the microscopic pore structure of concrete, it is found that the pore parameters also change with the process of freeze-thaw cycles. Therefore, in this section, the effects of air content, specific surface area, pore spacing coefficient, and average chord length on the macroscopic properties of concrete are analyzed by using the gray correlation method, and the factors that have the greatest influence on the macroscopic properties of concrete are obtained so that the macroscopic properties of concrete can be evaluated more comprehensively. In this way, the allows the macroscopic properties of the concrete to be evaluated more comprehensively.

4.1 Gray Correlation Analysis Method

Let the system behavior sequence be the following:

$$
\begin{aligned}
X_0 &= (x_0(1),\ x_0(2),\ \cdots,\ x_0(n)) \\
X_1 &= (x_1(1),\ x_1(2),\ \cdots,\ x_1(n)) \\
X_i &= (x_i(1),\ x_i(2),\ \cdots,\ x_i(n)) \qquad (16) \\
X_m &= (x_m(1),\ x_m(2),\ \cdots,\ x_m(n))
\end{aligned}
$$

For $\xi \in (0, 1)$, let

$$\gamma(x_0(k),\ x_i(k)) = \frac{\min_i \min_k |x_0(k) - x_i(k)| + \xi \max_i \max_k |x_0(k) - x_i(k)|}{|x_0(k) - x_i(k)| + \xi \max_i \max_k |x_0(k) - x_i(k)|} \tag{17}$$

$$\gamma(x_0,\ x_i) = \frac{1}{n}\sum_{k-1}^{n} \gamma(x_0(k),\ x_i(k)) \tag{18}$$

where ξ is the discrimination coefficient, and $\gamma(x_0, x_i)$ is called the gray correlation between X_0 and X_i.

The gray correlation is calculated as follows:

(1) Find the initial value of each sequence. Let

$$X_i^{\cdot} = \frac{X_i}{X_i(1)} = (X_i^{\cdot}(1), X_i^{\cdot}(2), X_i^{\cdot}(n)),\ \mathrm{i}\ =\ 0,\ 1,\ 2,\ \ldots,\ \mathrm{m} \tag{19}$$

(2) Find the absolute value sequence of the difference between the initial values of X_0 and X_i like the corresponding components, and write

$$\Delta_i(k) = |X_0^{\cdot}(k) - X_i^{\cdot}(k)|,$$

$$\Delta_i = (\Delta_i(1), \Delta_i(2),\ \ldots, \Delta_i(n)),\ \mathrm{i}\ =\ 0,\ 1,\ 2,\ \ldots,\ \mathrm{m} \tag{20}$$

(3) Find

$$\Delta_i(k) = |X_0^{\cdot}(k) - X_i^{\cdot}(k)|,\ \mathrm{k}\ =\ 0,\ 1,\ 2,\ \ldots,\ \mathrm{n},\ \ \mathrm{i}\ =\ 0,\ 1,\ 2,\ \ldots,\ \mathrm{m}$$

The maximum and minimum values, respectively, are denoted as

$$M = \max_i \max_k \Delta_i(k),\ m = \min_i \min_k \Delta_i(k)$$

(4) Calculate of the number of links

$$\gamma_{0i}(k) = \frac{m + \xi M}{\Delta_i(k) + \xi M},\ \xi \in (0,\ 1),\ \mathrm{k}\ =\ 0,\ 1,\ 2,\ \ldots,\ \mathrm{n},\ \ \mathrm{i}\ =\ 0,\ 1,\ 2,\ \ldots,\ \mathrm{m} \tag{21}$$

(5) Finally, the average of the correlation coefficients is found, i.e., the correlation degree

$$\gamma_{0i} = \frac{1}{n}\sum_{k=1}^{n} \gamma_{0i}(k),\ i = 0,\ 1,\ 2,\ \ldots,\ m \tag{22}$$

4.2 Relative Dynamic Modulus of Elasticity and Porosity Parameters

According to the above gray correlation method, the relative dynamic modulus of elasticity of concrete with fine aggregate from MSW incineration during freeze-thaw cycles was used as the reference column (Y), and the air content, specific surface area, pore spacing coefficient, and average chord length of pores were used as the comparison columns (X_1, X_2, X_3, and X_4) to investigate the degree of correlation between the relative dynamic modulus of elasticity and the pore parameters. The original series are listed in Table 11 below.

The original sequences of each test group in Table 11 were initialized to obtain Table 12. The original sequences of each test group in Table 11 were subjected to the different operations with the initial values of each sequence in Table 12, the absolute values were taken to obtain the absolute value sequences, and the correlation coefficients and correlation degrees were calculated, which are listed in Table 13 and Fig. 2.

Table 11: The original sequence of each experimental group

m_w/m_b	Sand replacement rate (%)	Index	Number of freeze-thaw cycles (cycles)				
			0 cycles	50 cycles	100 cycles	200 cycles	300 cycles
0.2	0	Y	100	99.14	98.25	98.17	97.20
		X_1	1.04	1.64	1.77	2.15	2.26
		X_2	25.78	42.83	40.38	37.11	30.19
		X_3	0.38	0.36	0.27	0.12	0.22
		X_4	0.13	0.10	0.09	0.08	0.06
	25	Y	100	99.55	99.15	96.99	95.23
		X_1	1.24	1.30	1.53	2.32	2.53
		X_2	42.39	68.13	59.68	56.97	44.61
		X_3	0.25	0.16	0.17	0.11	0.23
		X_4	0.11	0.07	0.08	0.07	0.12
	50	Y	100	98.68	98.22	97.95	96.20
		X_1	1.63	1.70	1.68	3.00	3.25
		X_2	49.56	86.18	79.31	65.66	56.86
		X_3	0.17	0.09	0.09	0.10	0.24
		X_4	0.10	0.05	0.05	0.06	0.09
0.4	0	Y	100	86.09	67.62	—	—
		X_1	1.14	1.90	2.17	—	—
		X_2	25.03	23.31	17.59	—	—
		X_3	0.38	0.21	0.35	—	—
		X_4	0.12	0.05	0.10	—	—
	25	Y	100	89.27	66.78	—	—
		X_1	1.25	1.99	2.71	—	—
		X_2	31.49	57.22	32.87	—	—
		X_3	0.35	0.14	0.26	—	—
		X_4	0.15	0.07	0.12	—	—
	50	Y	100	97.67	94.25	92.29	88.62
		X_1	1.52	1.49	1.81	1.93	2.29
		X_2	28.00	72.05	62.36	46.17	52.84
		X_3	0.31	0.28	0.25	0.08	0.30
		X_4	0.11	0.06	0.06	0.08	0.13

(Continued)

Table 11 (continued)

m_w/m_b	Sand replacement rate (%)	Index	Number of freeze-thaw cycles (cycles)				
			0 cycles	50 cycles	100 cycles	200 cycles	300 cycles
0.6	0	Y	100	79.95	—	—	—
		X_1	1.34	1.66	—	—	—
		X_2	63.46	47.50	—	—	—
		X_3	0.21	0.09	—	—	—
		X_4	0.09	0.04	—	—	—
	25	Y	100	67.14	—	—	—
		X_1	1.55	1.99	—	—	—
		X_2	31.33	40.81	—	—	—
		X_3	0.32	0.06	—	—	—
		X_4	0.12	0.04	—	—	—
	50	Y	100	91.18	87.35	—	—
		X_1	1.73	1.70	2.60	—	—
		X_2	47.42	57.83	38.71	—	—
		X_3	0.38	0.14	0.20	—	—
		X_4	0.11	0.07	0.12	—	—

Note: Unfilled data in the table indicate that the test specimen reached the freeze-thaw test stopping conditions and the test was stopped.

Table 12: Initial value image of each sequence

m_w/m_b	Sand replacement rate (%)	index	Number of freeze-thaw cycles (cycles)				
			0 cycles	50 cycles	100 cycles	200 cycles	300 cycles
0.2	0	Y	1	0.9914	0.9825	0.9817	0.9720
		X_1	1	1.5769	1.7019	2.0673	2.1731
		X_2	1	1.6614	1.5663	1.4395	1.1711
		X_3	1	0.9323	0.7109	0.3151	0.5677
		X_4	1	0.7760	0.7440	0.6160	0.4880
	25	Y	1	0.9955	0.9915	0.9699	0.9523
		X_1	1	1.0484	1.2339	1.8710	2.0403
		X_2	1	1.6072	1.4079	1.3439	1.0524
		X_3	1	0.6378	0.6732	0.4134	0.9094
		X_4	1	0.6491	0.7281	0.6316	1.0702
	50	Y	1	0.9868	0.9822	0.9795	0.9620
		X_1	1	1.0429	1.0307	1.8405	1.9939
		X_2	1	1.7389	1.6003	1.3249	1.1473
		X_3	1	0.5636	0.5455	0.6182	1.4788
		X_4	1	0.4554	0.5248	0.6337	0.9208

(Continued)

Table 12 (continued)

m_w/m_b	Sand replacement rate (%)	index	Number of freeze-thaw cycles (cycles)				
			0 cycles	50 cycles	100 cycles	200 cycles	300 cycles
0.4	0	Y	1	0.8609	0.6762	—	—
		X_1	1	1.6667	1.9035	—	—
		X_2	1	0.9313	0.7028	—	—
		X_3	1	0.5521	0.9063	—	—
		X_4	1	0.4180	0.8443	—	—
	25	Y	1	0.8927	0.6678	—	—
		X_1	1	1.5920	2.1680	—	—
		X_2	1	1.8171	1.0438	—	—
		X_3	1	0.4091	0.7273	—	—
		X_4	1	0.4444	0.7974	—	—
	50	Y	1	0.9767	0.9425	0.9229	0.8862
		X_1	1	0.9803	1.1908	1.2697	1.5066
		X_2	1	2.5732	2.2271	1.6489	1.8871
		X_3	1	0.9038	0.8077	0.2596	0.9647
		X_4	1	0.5179	0.5179	0.7411	1.1607
0.6	0	Y	1	0.7995	—	—	—
		X_1	1	1.2388	—	—	—
		X_2	1	0.7485	—	—	—
		X_3	1	0.4065	—	—	—
		X_4	1	0.4565	—	—	—
	25	Y	1	0.6714	—	—	—
		X_1	1	1.2839	—	—	—
		X_2	1	1.3026	—	—	—
		X_3	1	0.1807	—	—	—
		X_4	1	0.3471	—	—	—
	50	Y	1	0.9118	0.8735	—	—
		X_1	1	0.9827	1.5029	—	—
		X_2	1	1.2195	0.8163	—	—
		X_3	1	0.3770	0.5236	—	—
		X_4	1	0.6316	1.0877	—	—

Note: Unfilled data in the table indicate that the test specimen reached the freeze-thaw test stopping conditions and the test was stopped.

Table 13: Correlation coefficient between the relative dynamic elastic modulus and stomatal parameters

m_w/m_b	Sand replacement rate (%)	index	Number of freeze-thaw cycles (cycles)				
			0 cycles	50 cycles	100 cycles	200 cycles	300 cycles
0.2	0	X_1	1	0.5063	0.455	0.3562	0.3333
		X_2	1	0.4727	0.5071	0.5674	0.7510
		X_3	1	0.9104	0.6886	0.4739	0.5977
		X_4	1	0.7360	0.7157	0.6215	0.5537
	25	X_1	1	0.9114	0.6918	0.3765	0.3333
		X_2	1	0.4707	0.5664	0.5926	0.8446
		X_3	1	0.6033	0.6309	0.4943	0.9270
		X_4	1	0.6110	0.6737	0.6166	0.8219
	50	X_1	1	0.9019	0.9141	0.3747	0.3333
		X_2	1	0.4069	0.4550	0.5990	0.7358
		X_3	1	0.5494	0.5416	0.5881	0.4996
		X_4	1	0.4926	0.5300	0.5987	0.9260
0.4	0	X_1	1	0.4323	0.3333	—	—
		X_2	1	0.8971	0.9585	—	—
		X_3	1	0.6652	0.7273	—	—
		X_4	1	0.5808	0.7850	—	—
	25	X_1	1	0.5175	0.3333	—	—
		X_2	1	0.4480	0.6661	—	—
		X_3	1	0.6080	0.9265	—	—
		X_4	1	0.6259	0.8527	—	—
	50	X_1	1	0.9956	0.7628	0.6971	0.5627
		X_2	1	0.3333	0.3832	0.5237	0.4437
		X_3	1	0.9164	0.8555	0.5462	0.9104
		X_4	1	0.6350	0.6528	0.8145	0.7441
0.6	0	X_1	1	0.3333	—	—	—
		X_2	1	0.8116	—	—	—
		X_3	1	0.3586	—	—	—
		X_4	1	0.3904	—	—	—
	25	X_1	1	0.3793	—	—	—
		X_2	1	0.3722	—	—	—
		X_3	1	0.4327	—	—	—
		X_4	1	0.5358	—	—	—
	50	X_1	1	0.8262	0.3486	—	—
		X_2	1	0.5225	0.8549	—	—
		X_3	1	0.3864	0.4904	—	—
		X_4	1	0.5458	0.6112	—	—

Note: Unfilled data in the table indicate that the test specimen reached the freeze-thaw test stopping conditions and the test was stopped.

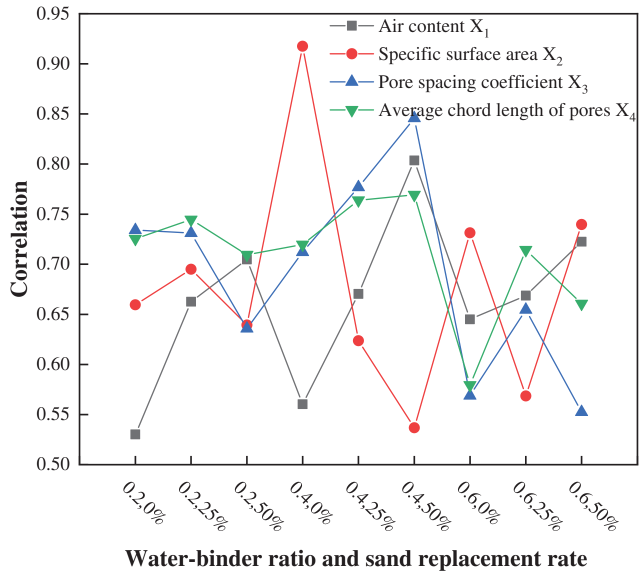

Figure 2: Correlation between the relative dynamic elastic modulus and stomatal parameters

As seen from Fig. 2, the pore parameters that have the greatest correlation with the relative dynamic modulus of the concrete with fine aggregates from MSW incineration are different for different ratios, The correlation between pore spacing coefficient and average pore chord length is high and relatively stable, and the correlation between air content and specific surface area is low and relatively unstable. The quantitative and qualitative analysis of the relative dynamic modulus of elasticity of the concrete is not comprehensive because, during the freeze-thaw cycle, the concrete undergoes complex structural changes, small pores gradually become large pores, cracks are created, and penetrated, and new pores are created.

4.3 Correlation Analysis of the Compressive Strength and Pore Structure

According to the above gray correlation method, the compressive strength of the concrete with fine aggregate from MSW incineration under freeze-thaw cycles was used as the reference column (Y), and the air content, specific surface area, pore spacing coefficient, and average chord length of pores were used as the comparison columns (X_1, X_2, X_3, X_4) to investigate the degree of correlation between the compressive strength and pore parameters. The correlation between the compressive strength and stomatal parameters was obtained using the same method as above.

The compressive strength decreases with increasing total pore volume and average pore diameter and increases with increasing specific surface area [27]. As seen in Fig. 3, the best correlation with the compressive strength value of concrete with fine aggregate from domestic waste incineration is the coefficient of pore spacing coefficient and the average pores chord length, and the relationship is similar to the relationship with the relative dynamic modulus of elasticity and pore parameters, indicating that for the compressive strength of the concrete, the size and number of pores have a greater degree of influence. When there are larger and more pores, the internal structure of concrete is looser, and the compressive strength will be reduced to a greater degree.

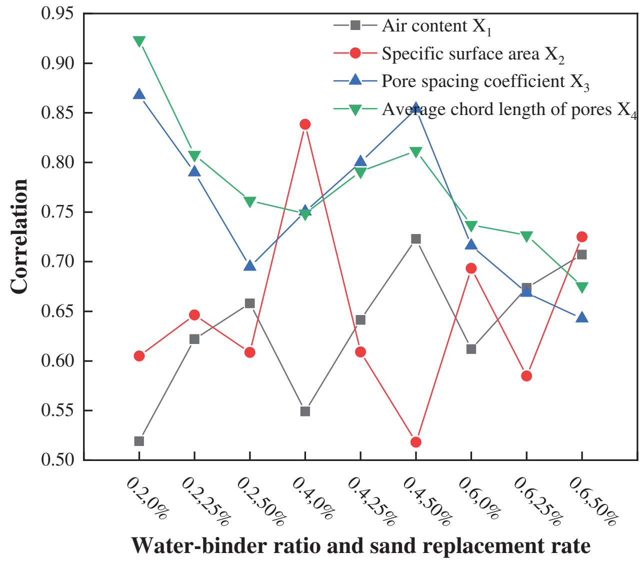

Figure 3: Correlation between the compressive strength and stomatal parameters

5 Conclusion

1. Based on the compressive strength of the fine aggregate concrete of MSW incineration bottom ash after freeze-thaw cycles, the gray mean GM (1,1) model was established to simulate the freeze-thaw process, and the simulated values were close to the actual values with relative errors less than 5%, and the accuracy of each group of models was one level, indicating that the mean GM (1,1) model can be well applied to the compressive strength of the fine aggregate concrete of MSW incineration bottom ash and can reflect its variation pattern more accurately.
2. Using the gray correlation method, the compressive strength and relative dynamic elastic modulus of the fine aggregate concrete from MSW incineration were correlated with the air content, specific surface area, pore spacing coefficient, and average pore chord length, and the compressive strength and relative dynamic elastic modulus were correlated with the pore spacing coefficient and average pore chord length. This indicates that the stomatal spacing coefficient and the average chord length of stomata are the main factors affecting the variations.

Funding Statement: This work is supported by the National Natural Science Foundation of China Project 51868058 and 52068058, Inner Mongolia Natural Science Foundation 2018MS05011, Inner Mongolia "Grassland Talent" CYYC5039.

Conflicts of Interest: The authors declare that they have no conflicts of interest to report regarding the present study.

References

1. Sawell, S. E., Chandler, A. J., Eighmy, T. T., Hartlén, J., Hjelmar, O. et al. (1995). An international perspective on the characterisation and management of residues from MSW incinerators. *Biomass and Bioenergy, 9(1),* 377–386. DOI 10.1016/0961-9534(95)00105-0.
2. Holbert, C., Lighty, J. S. (1998). Trace metals behavior during the thermal treatment of paper-mill sludge. *Waste Management, 18(6),* 423–431. DOI 10.1016/S0956-053X(98)00126-3.
3. Chen, J. C., Wey, M. Y., Lin, Y. C. (1998). The adsorption of heavy metals by different sorbents under various incineration conditions. *Chemosphere, 37(13),* 2617–2625. DOI 10.1016/S0045-6535(98)00161-1.

4. Rka, B., Hk, A., Sk, C., Svma, B. (2020). Hydrothermal liquefaction of biogenic municipal solid waste under reduced H_2 atmosphere in biorefinery format-sciencedirect. *Bioresource Technology, 310,* 123369–123377. DOI 10.1016/j.biortech.2020.123369.
5. Velusamy, S., Subbaiyyan, A., Ramasamy, K., Shanmugamoorthi, M., Vellingiri, V. et al. (2022). Use of municipal solid waste inert as a powerful replacement of fine aggregate in mortar cube. *Materials Today: Proceedings*, Tamil Nadu, India.
6. Yly, A., Jxl, A., Xiao, C. B., Ps, A., Haa, A. et al. (2022). Characteristics and production of semi-dry lightweight concrete with cold bonded aggregates made from recycling concrete slurry waste (CSW) and municipal solid waste incineration bottom ash (MSWIBA). *Journal of Building Engineering, 45,* 103434–103445. DOI 10.1016/j.jobe.2021.103434.
7. National Bureau of Statistics (2020). 2020 China national bureau of statistics data domestic waste removal volume. https://data.stats.gov.cn/easyquery.htm?cn=C01&zb=A0B09&sj=2020.
8. National Bureau of Statistics (2020). 2020 China national bureau of statistics data waste incineration harmless treatment volume. https://data.stats.gov.cn/easyquery.htm?cn=C01&zb=A0C06&sj=2020.
9. Cao, X. G. (2009). *Research on application of municipal solid waste combustion residues for freeway pavement base* (*Master Thesis*). Nanjing University of Aeronautics and Astronautics, China.
10. Qian, S., Lin, J., Tang, B. S. (2014). Preparation of glass foams from vitrified municipal solid waste incinerator ash. *Journal of the Chinese Ceramic Society, 42(1),* 108–112.
11. Lin, S. Y. (2021). *Experimental study on carbonation and chloride ion penetration of fine aggregate concrete from municipal solid waste incineration ash* (*Master Thesis*). Inner Mongolia University of Technology, China.
12. Huang, Y. (2021). *The study on mechanical properties of simulating component of concrete project with MSWI as fine aggregate* (*Master Thesis*). Inner Mongolia University of Technology, China.
13. Xu, K. D., Wang, J. N., Chen, J. L., Li, Z. X., Niu, J. S. et al. (2019). Judge of properties of household waste incineration ash residue and its risk of environmental safety. *Non-Metallic Mines, 42(6),* 90–93.
14. Shi, D. S., Liu, S. J., Song, J. Z. (2021). Experiment of mix design and mechanical properties about concrete using MSW bottom slag as fine aggregate. *Concrete, 2021(3),* 145–8 + 52.
15. Song, Y. F., Deng, C. J., Zhu, H. X., Ding, J., Zhang, X. J. (2016). Correlation between porosity characteristics and cold crushing strength of forsterite porous materials based on grey system theory. *Journal of Silicates, 44(6),* 896–900.
16. Deng, J. L. (1990). *A tutorial on gray systems theory.* China: Huazhong University of Science and Technology Press.
17. Liu, S. F. (2010). *Gray system theory and its applications*. China: Science Press.
18. Guo, Z. Q., Zhao, K., Xie, L., Xiao, H. P. (2012). Grey prediction of dynamic modulus of elasticity of concrete under complex environment. *Railway Engineering, 2012(10),* 150–153.
19. Li, B. X., Cai, L. H., Zhu, W. Z. (2018). Predicting service life of concrete structure exposed to sulfuric acid environment by gray system theory. *International Journal of Civil Engineering, 16(9)*, 1017–1027. DOI 10.1007/s40999-017-0251-2.
20. Li, B., Cai, L., Wang, K., Zhang, Y. (2016). Prediction of the residual strength for durability failure of concrete structure in acidic environments. *Journal of Wuhan University of Technology-Mater Science Edition*. *31(2),* 340–344. DOI 10.1007/s11595-016-1373-0.
21. Yin, Y., Fan, Y., Ning, W. (2018). Research on the prediction of mechanical response to concrete under sulfate corrosion based on the gray theory. *IOP Conference Series: Earth and Environmental Science, 153(2)*. Guang Xi, China.
22. Mehta, P. K. (1991). Concrete durability-fifty years progress. *Proceedings of 2nd International Conference on Concrete Durability*, pp. 1–32. Montreal, Canada.
23. Xu, J. N., Liu, Z. X., Liu, H. X. (2018). Experimental study on bond strength of fiber recycled concrete and BFRP Bar under freeze-thaw cycles. *Bulletin of the Chinese Ceramic Society, 37(10),* 3355–3360.
24. Yazdani, F. (2015). *Damage assessment, characterization, and modeling for enhanced design of concrete bridge decks in cold regions* (*Master Thesis*). North Dakota State University, USA.

25. Zhao, Y. R., Liu, F. F., Wang, L., Guo, Z. L. (2020). Modeling of the compressive strength of basalt fiber concrete based on pore structure under single-side freeze-thaw condition. *Materials Reports, 34(12),* 12064–12069.
26. Chu, H. Q., Jiang, L. H., Zhang, Y. (2010). Forecast of carbonation of concrete after electrodeposition treatment based on grey theory. *Journal of Hohai University (Natural Sciences), 38(2),* 170–175.
27. Luo, B. B., Bi, Q. W. (2012). Experimental study on the influence of pore structure of hybrid fibers self-compacting concrete on compressive strength. *Bulletin of the Chinese Ceramic Society, 31(3),* 626–630.